Kink kinetics, exchange fluxes, 1D `nucleation' and adsorption on the (010) face of orthorhombic lysozyme crystals

1999 J. Phys.: Condens. Matter 11 9969

(http://iopscience.iop.org/0953-8984/11/49/314)

J. Phys.: Condens. Matter **11** (1999) 9969–9984. Printed in the UK PII: S0953-8984(99)04150-8

Kink kinetics, exchange fluxes, 1D 'nucleation' and adsorption on the (010) face of orthorhombic lysozyme crystals

A A Chernov†§, L N Rashkovich‡, I V Yaminski‡ and N V Gvozdev‡

† Universities Space Research Association/NASA/Marshall Space Flight Center, 4950 Corporate Drive, Suite 100, Huntsville, AL 35805, USA

‡ Physics Department, Moscow State University, Moscow, Vorobyevy Gory, 117234 Moscow Russia

E-mail: alex.chernov@msfc.nasa.gov and rashk@polc49.phys.msu.su

Received 10 May 1999

Abstract. Rare kinks (1.74×10^{-3} kinks nm^{-1}) on the otherwise molecularly straight ⟨001⟩ growth steps on the (010) face of orthorhombic lysozyme were studied. These straight steps are generated at the edge between the (010) and (110) faces. Each step is assumed to propagate by creation of one-dimensional (1D) 'nuclei'—the segments of a new molecular rows irreversibly attached to the straight step in the course of a trial and error process. Each 'nucleus' is built of two neighbouring unit cells and is thus limited by two kinks possessing opposite signs. The steps move along the face at a rate ∼0.19 nm s^{-1}, at relative supersaturation about unity. Kink statistics and step rate measurements allowed us to evaluate the velocity of the kink along the step to be 19.3 nm s^{-1}, and corresponding average frequencies at which attachment to and detachment from a kink occur to be ≃50 and 25 molecules s^{-1}, respectively. The rate at which the 1D 'nuclei' appear at a step was found experimentally to be $J = 2.7 \times 10^{-5}$ nm^{-1} s^{-1}.

This rate was also calculated as a probability that a sole molecular species adsorbed at the otherwise straight step will stay there forever. The rate of an arbitrarily oriented step driven by the 1D nucleation was also theoretically found to have a non-singular minimum at the close-packed orientation. On this theoretical basis, the coverage of the ⟨001⟩ step by unit cells was extracted from experimental data to be 6.5×10^{-6}. Taking into account translational, rotational and vibrational partition functions flat face coverage with adsorbed molecules was estimated. The calculated adsorption coverage fits with the experimental data if the molecular detachment energy from a kink is ∼6.6 kcal mol^{-1}. The terrace adsorption coverage is $\sim 10^{-3}$.

The same approach is used to outline simple equations for protein solubility. The predicted solubility either rises with rising temperature—at a higher ratio of intermolecular binding energy to kT—or diminishes as the temperature rises—in the opposite case. The latter retrograde solubility comes from a high entropy loss associated with crystallization.

1. Introduction

The most elementary act of crystal growth is attachment of a molecule, atom or an ions to the lattice at the kink position [1–5]. The rate of this process may be experimentally evaluated from the step rate and kink density. Kink visualization has not been achieved for inorganic crystal growth so far. Therefore only the step kinetics was quantitatively evaluated [6–8]. However, essentially straight steps thus possessing low kink density have been observed on, e.g., calcite and phosphates by atomic force microscopy (AFM) [9–11]; these steps are supposed to proceed by one-dimensional nucleation of kink pairs and nevertheless comply

§ Corresponding author.

0953-8984/99/499969+16$30.00

with the Gibbs–Thomson law [9, 10]. Such compliance, generally speaking, is not necessarily at high supersaturation [12, 18]. Though molecular resolution has been achieved on, e.g., dicalcium phosphate [11] single kinks were not clearly observed. However, high resolution achieved on biomolecular crystals of at least an order of magnitude larger unit cells [14] opens the way to study single kink behaviour. Recently, AFM allowed observation of the movement of a single kink on growing thaumatin [15] and on lysozyme [16]. These observations suggest that a molecularly straight step moves by one-dimensional nucleation of which the theory for simple Kossel crystal was addressed earlier [17–22]. Analysing the kink statistics and step kinetics, one may evaluate elementary frequencies of molecular attachments to the kinks and the rate of 1D nucleation. The kink, i.e. half-crystal position [1–5], can be easily identified in the simple lattices. However, in a complex lattice built of one or several types of molecule or of various ions, these elementary species present in solution separate from one another are often not in equivalent positions within the unit cell. Correspondingly, the steps which are a fraction of the lattice spacing height are relatively rare though they were observed even in simple lattices, e.g. on the (100) Ag face. Most often, however, the step height equals the full lattice spacing. In these cases, detachment of different elementary species from the crystal is associated with breaking different bonds, so that only the unit cell as a whole may occupy a real kink, the half-crystal position. Actual steps on such a crystal would contain various partially filled cells in the kink position, evidently following the Gibbs distribution. The general concept and inevitable existence of the partially filled kinks is clear [13]. However, for complex lattices, the growth and nucleation events need special consideration, which is still missing.

In this paper, we first present experimental data on kink observations (sections 2, 3) and statistics (section 4), then theoretically outline the rate of 1D nucleation for the Kossel crystal making use of the conservation probability concept [23]—a different approach from that employed earlier by Voronkov [17, 18] (section 5) and the rate of an arbitrarily oriented step growing by 1D nucleation (section 6). Analysing, on this basis, the measured step rate we extract the experimental kink rates, molecular fluxes in and out at the kinks, the 1D nucleation rate (section 7) and kinetic coefficients (section 8). The 1D nucleation rate allows us to estimate step coverage by unit cells (section 7). In section 9, simple adsorption and solubility equations are derived by taking into account translational, rotational and vibrational entropies in the ideal gas approximation. Confronting these equations with the experimental data, molecular attachment energies and terrace coverages are evaluated. A summary is given in section 10.

2. Experiment

Hen egg white lysozyme, HEWL (Seikagaku, Japan) crystals were obtained employing spontaneous nucleation and growth by lowering temperature in an aqueous solution of 5 mass% of HEWL, 5 mass% of NaCl at pH $= 4.6$. This acidity was adjusted by adding HCl. The crystals shown in figure 1 are similar to the ones described earlier [24].

The most developed {010} face was investigated in the Nanoscope III Digital Instruments Atomic Force Microscope (AFM) in the constant force mode. In the AFM, the silicon mitride tips have the apex angle of 36°. Scanning frequency was 10 Hz, 512 lines per frame. Molecular resolution was achieved only with a small force, $\sim 10^{-10}$ N applied to the sample. At a larger force, the surface is damaged. When probing the crystal edges, we used a wide range of scanning angles. A crystal on a glass substrate was placed in a standard cuvette with solution. In our experiment conducted at 25 °C and discussed here, the supersaturation $\sigma \equiv C/C_e - 1$ was estimated to be close to 1, where C and C_e are the actual and equilibrium concentrations

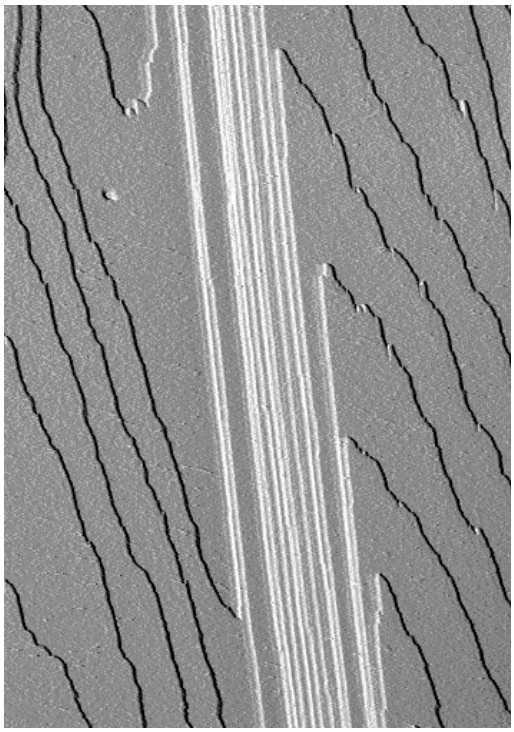

Figure 1. AFM images of steps on the (010) face. Straight white steps are parallel to the c-axis, $\langle 001 \rangle$, and are moving to the left. Dark zigzag wavy steps are moving to the right.

respectively, with C_e determined from the solubility curve in [25]. The crystal structure is described by the space group $P2_12_12_1$ and according to the x-ray determinations [26, 27] has lattice spacing, $a = 5.65$ or 5.64, $b = 7.39$ or 7.37, $c = 3.05$ or 3.04, respectively.

3. Step Sources

Typically, on the (010) face of orthorhombic lysozyme, the steps are generated by dislocation and, very rarely, by two-dimensional nucleation. Steps on the surface are strongly anisotropic (figure 1): these are straight when moving to the left in figure 1 (white contrast), while they acquire various orientations when propagating to the right (dark contrast). The steps studied in this work were exclusively split from the excrescence (figure 2) formed along the whole edge between the (010) and (110) faces due to unknown reasons, probably high supersaturation. The excrescence slope provides a train of practically parallel steps on the (010) face moving in one direction only (figure 3) corresponding to the white contrast in figure 1. The dislocations and 2D nucleation sources were suppressed by this train. Such a train is shown in figure 3 in which figure 3(b) is taken 304s later than figure 3(a). The corresponding step rate was measured to be $v_{st} = 0.19$ nm s^{-1}.

4. Kink images and statistics

Figure 4 shows one single kink on a step (black line) between the upper terrace on the right and lower terrace on the left. The periodical lattice cell rows are seen on both terraces. The kink height measured in the horizontal direction follows from the step shift and thus equals one lattice spacing along the a-axis. The experimental resolution in the 9×9 μm^2 image

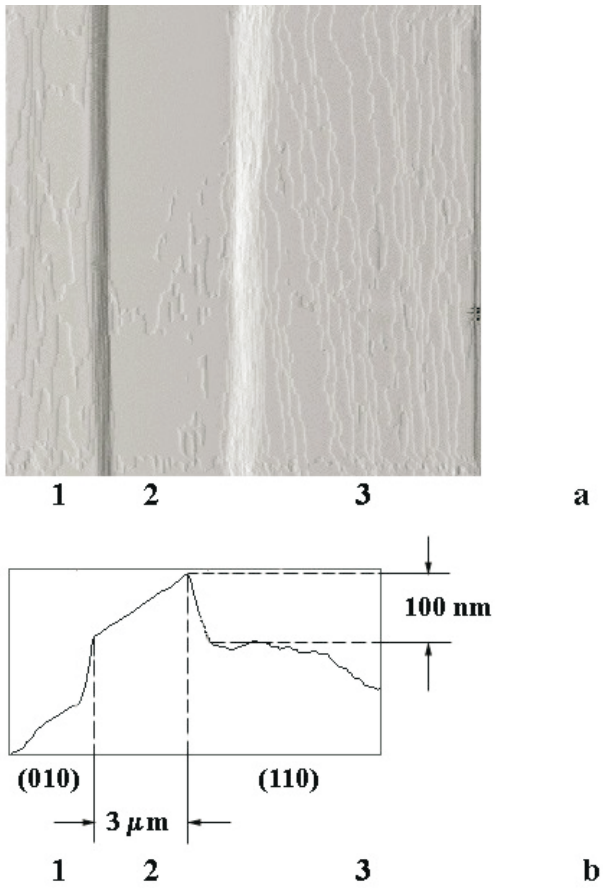

Figure 2. Top (a) and side (b) views of the flat-top excrescence on the ⟨001⟩ edge between the (110) and (010) faces. The excrescence is the only source of the steps on the (010) face under consideration.

is 9×10^3 nm/512 = 17.6 nm, since the image is built of 512 × 512 blocks. Thus a kink extended by about 17.6 nm was considered as single, while deeper ones were identified as double, triple etc, depending on the kink height. Fortunately, these complex kinks are rare and do not influence kink statistics essentially.

In figure 3, a kink moving down along a step, is named positive, '+'; the one moving up is negative, '−'. The kink statistics are presented in table 1. The + and − kinks are supposed to nucleate by pairs at random on the step and then disappear by mutual annihilation, also at random points on the steps. We assume that the nucleation occurs at the same rate on the straight, kink free segments ij between two kinks of any type, $i, j = +, -$. The same is expected to be true for the annihilation points if velocities of all kinks are constant. Under these assumptions, the position of the + and − kinks on a step should not be correlated. Therefore, the average lengths, $x_{ij}(i, j, = +, -)$, of segments between any kinks i and j should be equal to one anther, i.e. independent of ij:

$$x_{ij} = 1/(n_+ + n_-). \tag{1}$$

The randomness means the Poisson distribution of the interkink distances. In other words, the probability that a segment of a length x does not contain any kink is:

$$P(x) = \exp[-(n_+ + n_-)x]. \tag{2}$$

Thus the relative number of kinks separated by a distance x, such that $x_1, < x < x_2$ is

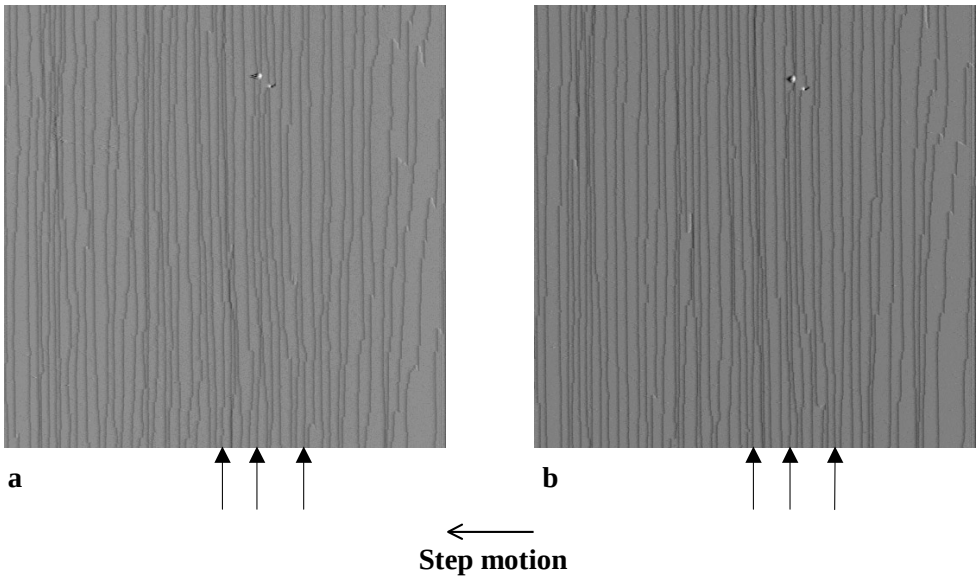

Figure 3. Two subsequent 9×9 μm^2 AFM images of the $\langle 001 \rangle$ steps, all moving to the left, the frame a was taken 304 s earlier than b. The kinks statistics (see table) was collected on the three steps marked by the arrows.

$\exp[-(n_+ + n_-)x_1] - \exp[-(n_+ + n_-)x_2]$. The corresponding histogram in figure 5 presents the cumulative percentage of pairs of any kind possessing lengths within the ranges 0–200, 200–400, ..., 1400 + 600 nm, with $n_+ + n_- = 1.74 \times 10^{-3}$ nm^{-1}, i.e. $x_{ij} = 575$ nm. The probability (2) and histogram in figure 5 are normalized to the total number of pairs, evidently equal to the total number of kinks, =269. The overall distribution of all segment lengths, x, according to figure 5, seems to be Poissonian with sufficient accuracy, the experimental number of pairs found within the intervals 0–200, 200–400, ..., 1400–1600 nm are, respectively, 80, 54, 34, 27, 23, 17, 9, 12 with 13 segments exceeding the length of 1600 nm. Thus the accuracy of ∼30% at the tail of the Poisson distribution in figure 5 does fit an estimate of the inverse root square of the number of observed pairs.

Table 1. Statistics of kinks.

Types of kinks, $i = +, -$ and interkink segments ij, $i, j = +, -$	Total number of kinks and segments	Probabilities	Linear densities of kinks and segments n_i, n_{ij}, 10^{-3} nm^{-1}	Average interkink distance $\langle x_{ij} \rangle$ nm	σ (dispersion, distribution of the x_{ij})$^{1/2}$ nm	$\frac{n_i n_j}{n_+ + n_-}$ 10^{-3} nm^{-1}
Total	269		1.74	575 ± 36	589 ± 25	
+	172[a]	0.639	1.11			
−	97[b]	0.361	0.672			
++	123	0.457	0.796	567 ± 49	541 ± 35	0.711
+−	49	0.182	0.317	529 ± 109	766 ± 77	0.401
−+	50	0.186	0.186	860 ± 61	430 ± 43	0.401
−−	47	0.175	0.304	418 ± 79	539 ± 79	0.226

[a] including 10 double, 6 triple and 1 quadruple kinks.
[b] including 7 double and 4 triple kinks.

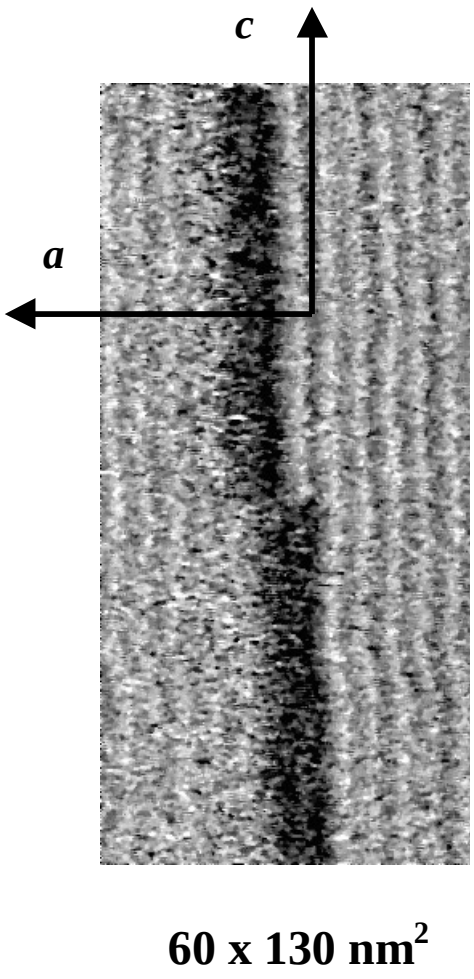

Figure 4. Single kinks on the step showing black contrast in figure 1. Left terrace is ∼7 nm lower than the left. Molecular rows are seen on both terraces. The kink is supposed to be one lattice spacing deep, $a = 5.65$ nm deep.

The dips on a step, i.e. the segments $+-$, are on average noticeably shorter than the bumps: $x_{+-} = 529$ while $x_{-+} = 860$ nm. This asymmetry is in contrast with the much better balance between probabilities to meet a dip versus bump: $p_{+-} = 0.182$ versus $p_{-+} = 0.186$ ($p_{+-} + p_{-+} + p_{++} + p_{--} = 1$, see table 1). If this disparity between the x_{+-} and x_{-+} is not a result of insufficient statistics, one may think of an impurity as a reason: if the impurity is pushed by kinks it should accumulate in the dips (the x_{+-} segments) and thus decrease the kink rate.

We shall go on with the kink and step kinetics after the outline of one-dimensional (1D) nucleation rate and the corresponding step rate required for this analysis.

5. One-dimensional nucleation

There are two ways to create kinks on an originally straight step of singular orientation parallel to the chain of the strongest intermolecular bonds. The first presumes an 'open system'—adsorption of molecules from the surrounding solution, vapour, 2D adsorption layer or melt at the straight step rise, attachment of the next molecules to these new kinks and reverse flux

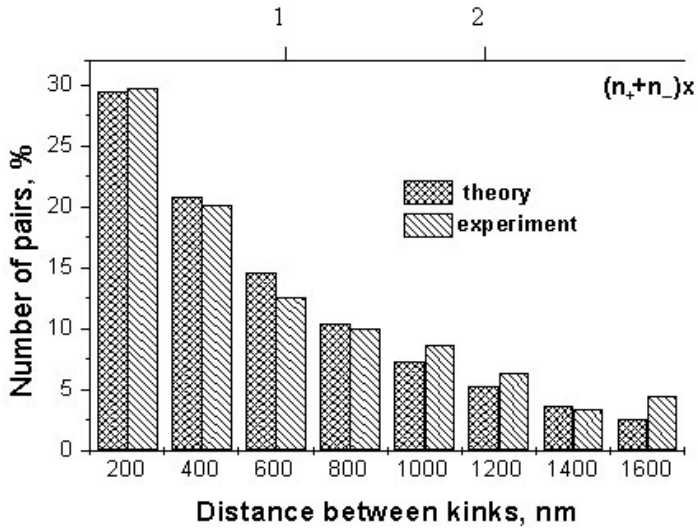

Figure 5. Distribution of the interkink segments over their lengths. Theoretical data follow Poisson distribution.

of desorption and detachment of molecules from the adsorption position at the step and from the kinks. The other way is rearrangement of molecules already making the step riser. The latter conservative 'closed system' does not assume exchange with the surroundings [4]. Both open and closed system mechanisms of the step shape fluctuations should result in the same kink density at thermodynamic equilibrium. This equilibrium kink density is proportional to $\exp(-\varepsilon/kT)$ where ε is the kink energy [4, 5] and should be low at low kT/ε ratio. Noticeable deviation from equilibrium, typical of protein crystal growth, demands special consideration to find the kinetic kink density and is addressed below. During steady state crystal growth, the kinks of opposite signs annihilate at the rate at which the new kinks are generated. The kink generation rates in the open and the closed systems are different. For instance, on a $\langle 100 \rangle$ step on a (001) face of a simple cubic lattice (Kossel crystal) relocation of a molecule from the position 'in the step' to the position 'at the step' requires breaking four bonds between nearest neighbours: three in the same layer and one in the layer below. This will lead to creation of four kinks at once. If the bond strength is $\varepsilon_0 = 2\varepsilon$, the frequency of relocation is proportional to $\exp(-8\varepsilon/kT)$ and should be low at the low (kT/ε) ratio. In contrast, adsorption from the surroundings, though it may require overcoming a dehydration and entropic barrier higher than that on the conservative way, does not presume breaking of the intermolecular bonds, and thus is expected to be faster, at sufficiently low (kT/ε) ratio. Thus, the kinetic step roughness is different from the equilibrium one and depends on the roughening mechanism.

As soon as the conservative fluctuation rate is low, creation of one-dimensional (1D) nuclei by adsorption is of major importance. This process was first addressed by Voronkov [18]. Here we use a different, even simpler approach to outline the 1D nucleation rate, following [22] and [23]. Before doing so, we should realize the distinction between the simple cubic model typically used and the real complex lattice. The unit cell of the orthorhombic lysozyme is shown in figures 6(a) and (b), in two projections. As it is discussed below in section 9, it reminds us of the simple cubic packing since each molecule has six nearest neighbours [26, 27]. The fact that only single kinks one unit cell wide are observed indicates

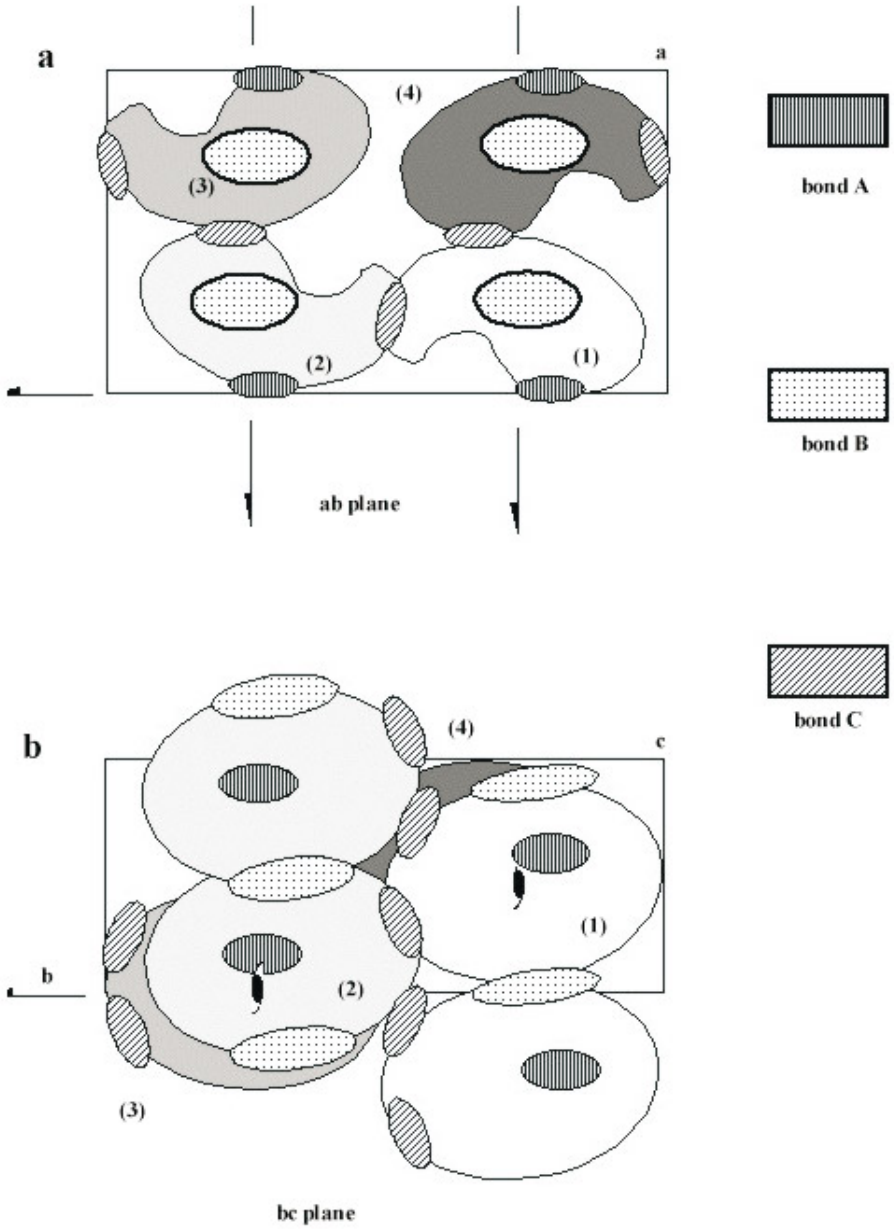

Figure 6. Schematic views of the orthorhombic lattice unit cell: a—viewed along the *c*-axis, b—viewed along the *a*-axis. The relative strengths (kcal mol^{-1}) of the contacts A, B, C were estimated to be 70:46:31 by multiplying the numbers of the direct and water-mediated hydrogen bonds and van der Waals bonds in each contact by the energies of 3, 1.5 and 0.3 kcal mol^{-1} per each of these bonds, respectively [27]. In the approximation by cubic lattice, still only the unit cell of four molecules makes the real kink and is considered as a growth unit for 1D nucleation. Averaging the molecular states over the unit cell allows to introduce the effective binding energy $2\varepsilon_0$ for the single adsorbed molecule 'Mol' in figure C, $4\varepsilon_0$ for the adsorbed 'cell' and $3\varepsilon_0$ for the single molecule '1' in the pseudo-kink position.

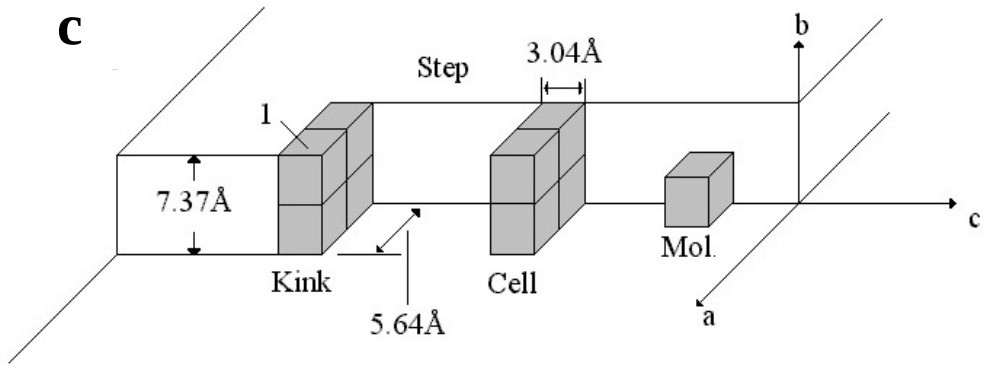

Figure 6. (Continued)

stronger binding within the unit cell than along the single rows parallel to the step, so that separate rows of molecules, unlike thaumatin [15], are not deposited. However, at this point, we only note that the 1D nuclei at the step should be made of two unit cells, i.e. of eight molecules, and that the kink is built by the unit cell. Therefore, we will consider the cell as the only growth unit. In sections 7 and 9 we shall qualitatively take into consideration that each of these unit cells should be built by attachments and detachments of single molecules.

We denote ultimate frequencies at which the whole unit cell appears and disappears at the step by w_{+a} and w_{-a}, respectively. The sole absorbed unit may be joined from its both sides by the next one at the frequency w_+ of attachment to a kink. Detachment from a kink occurs at the frequency w_-. Binding in the kink is stronger than at the step. Therefore, $w_{-a} \gg w_-$. At equilibrium, $w_+ = w_-$. In supersaturated solution, $w_+ > w_-$.

As soon as the adsorbed unit is joined by the next similar one, each of them may be detached at the frequency $w_- \ll w_{-a}$, which inequality makes the pair more stable than a single unit. Attachment of the third, fourth etc unit from any side of the 'one-dimensional' cluster makes it even more stable and raises the chance that the first adsorbed unit and its neighbour become a 1D nucleus, i.e. stay forever. The probability of this event of ultimate conservation of the unit once it has appeared is designated as C_1. Similarly, probabilities that a once formed pair, triplet etc, of units will stay forever are C_2, C_3, ... Thus, out of N single adsorbed units, NC_1 will stay forever. On the other hand, out of these N units Np_1 will be joined by the next unit from either of two sides, where

$$p_1 = 2w_+/(2w_+ + w_{-a}). \tag{3}$$

Out of these Np_1 pairs, Np_1C_2 will ultimately stay forever after the first attachment of the second unit because, by definition, C_2 is the probability that a pair, once formed, will stay forever. The remaining $Np_1(1 - C_2)$ pairs will lose the second unit and come back to one adsorbed unit, i.e. to the initial state. This state is conserved at probability C_1. Therefore $Np_1(1 - C_2)C_1$ units will be conserved after third, fourth etc attempts. Thus,

$$C_1 = p_1C_2 + p_1(1 - C_2)C_1 \qquad \text{or} \qquad C_1 = p_1C_2/[1 - p_1(1 - C_2)]. \tag{4}$$

Similarly,

$$C_2 = pC_3/[1 - p(1 - C_3)] \qquad C_n = pC_{n+1}/[1 - p(1 - C_{n+1})]$$
$$n = 2, 3, \ldots \qquad p = w_+/(w_+ + w_-). \tag{5}$$

For sufficiently long segments, $n \gg 2$, one should expect $C_n = C_{n+1}$. Then (5) gives

$$C_2 = C_3 = \cdots = C = [p - (1 - p)]/p = (w_+ - w_-)/w_+. \tag{6}$$

Substituting C_2 from equation (6) into equation (4) and taking into account that w_{+a}/c adsorbed units appear per unit step length per unit time one obtains the 1D nucleation rate

$$J = (w_{+a}/c)C_1 = 2(w_{+a}/c)(w_+ - w_-)/[w_{-a} + 2(w_+ - w_-)] \tag{7}$$

coinciding with the result of [17]. In [22] conservation of a pair was considered rather than one unit. Therefore equation (7) is more relevant for 1D nucleation, though conservation of four molecules might be relevant to find the frequency of appearance of the growth unit, w_{+a}.

6. Step rate

As soon as the 1D nucleation rate, J, is known we may calculate the rate of an arbitrarily orientated step. A step strictly singular on average was considered in [17–21]. Let us consider a step, deviated on average, from singular orientation by an angle φ counted anticlockwise. Then

$$n_+ - n_- = a^{-1} \tan\varphi \tag{8}$$

where n_+ and n_- are the kink densities (section 4) and a is the lattice spacing along the a-axis normal to the step. The kinks are born and mutually annihilate by pairs. Therefore

$$J = 2v_k n_{+-}/x_{+-} = 2v_k n_+ n_- \qquad \text{since} \qquad x_{+-} = x_{-+} = x_{++} = x_{--} = (n_+ + n_-)^{-1}. \tag{9}$$

Combining equations (8) and (9) one obtains the kink densities, n_+, n_-, and step rate, v_{st}:

$$an_\pm = (1/2)\{[(\pm\tan\varphi) + [(\tan\varphi)^2 + 2a^2 J/v_k]^{1/2}\} \tag{10}$$

$$v_{st} = (n_+ + n_-)av_k = [(v_k \tan\varphi)^2 + 2a^2 v_k J]^{1/2}. \tag{11}$$

Naturally, the step rate is minimal at $\varphi = 0$. This minimum is smooth rather than singular, as it should be for a fluctuating one-dimensional object, similar to the step energy anisotropy. However, on our moving step, the fluctuations are of non-equilibrium, kinetic nature.

A step possessing the form of a loop and expanding at a constant rate v_{st} from a nucleus formed at the time $t = 0$ should by the time t have radius of curvature $R(\varphi) = (v_{st} + \partial^2 v_{st}/\partial\varphi^2)t$ [5]. At $\varphi = 0$, $R = R_0 = v_{st}[1 + (v_k/v_{st})^2]t \simeq (v_k^2/v_{st})t$ if $v_k \gg v_{st}$. This relation may provide another tool to determine the kink rate. In our experiment, however, all the considered steps generated by edge excrescence were straight (figure 3) and did not form closed loops.

7. Propagation and nucleation rates of kinks. Exchange fluxes

According to the first of equations (11), one can find the kink velocity, v_k, if the step rate, v_{st}, and the total kink density, $n_+ + n_-$, are known experimentally. In our experiment, $v_{st} = 0.19 \pm 0.04$ nm s^{-1}, $n_+ + n_- = 1.74 \times 10^{-3}$ nm^{-1}, $a = 5.65$ nm, so that $v_k = 19.3 \pm 4.1$ nm s^{-1}, i.e. it is $1/a(n_+ + n_-) \simeq 100$ times the average step rate. The kink rate may be expressed via the elementary frequencies of the new cell formation w_+, or dissolution, w_- at the kink site:

$$v_k = c(w_+ - w_-) = cw_-\sigma \equiv \beta_k\omega(C - C_e)$$

$$\sigma = (w_+ - w_-)/w_- = (C - C_e)/C_e. \tag{12}$$

Here β_k is the kinetic coefficient for a kink and ω is the volume of a molecule. It is related to the measured step kinetic coefficient $\beta_{st} = v_{st}/\omega(C-C_e)$ as $\beta_k = \beta_{st}/a(n_+ + n_-)$ (section 8). The relative supersaturation σ should be expressed via the actual and equilibrium protein activities approximated here by the corresponding concentration, C and C_e. Taking $c = 3.05$ nm, $v_k = 19.3$ nm s^{-1}, $\sigma = 1$ we obtain from equation (12) the unit cell fluxes w_-, w_+ from and to a kink, respectively:

$$w_- = v_k/c\sigma = 6.3 \text{ units s}^{-1} \qquad w_+ = (1+\sigma)w_- = 12.6 \text{ units s}^{-1}. \tag{13}$$

Displacement of a kink by the cell length c means filling the unit cell consisting of four molecules. Then the molecular attachment and detachment frequencies w_{+m}, averaged over the cell, are

$$w_{+m} = 4w_+ = 50.6 \text{ molecules s}^{-1} \qquad w_{-m} = 25.3 \text{ molecules s}^{-1}. \tag{14}$$

The 1D nucleation rate follows from equation (11) with $v_k = 19.3$ nm s^{-1}, $n_+ = 1.11 \times 10^{-3}$ nm^{-1}, $n_- = 0.627 \times 10^{-3}$ nm^{-1} (see table 1):

$$J = 2.7 \times 10^{-5} \text{ nm}^{-1} \text{ s}^{-1} = 2.7 \times 10^2 \text{ cm}^{-1} \text{ s}^{-1}. \tag{15}$$

With these J, v_k, n_+, n_- one can ignore the angular deviation term $(\tan\varphi)^2$ in equations (10) and (11).

As mentioned in section 7, one may expect $w_{-a} \gg w_-$ and $w_{-a} \gg w_+ - w_-$. Then with $c = 3.05$ nm one obtains the coverage θ of the step by adsorbed unit cells from equation (7):

$$\theta = w_{+a}/w_{-a} = Jc/2(w_+ - w_-) = 6.5 \times 10^{-6}. \tag{16}$$

If $w_{-a} < 2(w_+ - w_-)$ then equation (7) gives $w_{+a} \simeq Jc \simeq 8 \times 10^{-5}$ s^{-1} which is in contradiction with the natural expectation that w_{+a} is of the order of w_+ given by equation (13).

8. Kinetic coefficients

The kinetic coefficients of steps and kinks, β_{st} and β_k, are defined in and immediately after equation (12). At the measured $v_{st} = 0.19 \times 10^{-7}$ cm s^{-1}, $n_+ + n_- = 1.74 \times 10^4$ cm^{-1}, $a = 5.65 \times 10^{-7}$ cm, $C = 2.09 \times 10^{18}$ cm^{-3}, $C_e = 1.05 \times 10^{18}$ cm^{-3}, $\omega = 3 \times 10^{-20}$ cm^3 one obtains $\beta_{st} = 6.03 \times 10^{-7}$ cm s^{-1}, $\beta_k = 6.14 \times 10^{-5}$ cm s^{-1}.

Figures for comparison follow from the kinetic coefficient for steps on the (101) face of tetragonal lysozyme, $\beta_{st} = 4.6 \times 10^{-5}$ cm s^{-1} [7]. It was found by first interferometric measurements of the effective step rates as a function of logarithmic supersaturation, $\ln C/C_e$, to be 2.8×10^{-4} cm s^{-1} and recalculated for the absolute supersaturation $(C - C_e)$ at $C/C_e = 5.47$ ([33], p 344). The interferometrically observed dislocation hillocks were clearly round suggesting that the interkink segments were not more than 2–3 intermolecular distances long. Therefore, for the data of [7] one may expect $\beta_k \simeq 2 \times 10^{-5}$ cm s^{-1} which is not far from 6.1×10^{-5} cm s^{-1} in this work as would be expected for the same molecules. The difference, again, may come from different molecular packing in the crystal bulk, step and kink. It is an open question to what extent attachment and detachment frequencies are different for different positions in the unit cell.

The Brownian frequency, ν, at which molecules attack kinks or other molecular sites may be approximated as:

$$\nu \simeq C\omega^{2/3}(kT/2\pi m)^{1/2} \simeq 10^8 \text{ s}^{-1}, \tag{17}$$

with $C = 2.09 \times 10^{18}$ cm^{-3}, the surface per molecule site area $\omega^{2/3} \simeq 10^{-13}$ cm^2 and the average Brownian impinging velocity $(kT/2\pi m)^{1/2} \simeq 5.2 \times 10^2$ cm s^{-1}. Having in mind frequencies in equation (14), one should conclude that only one of about 10^6 protein molecules

trying to enter the lattice succeeds. This supports the necessity of the pre-kink selection of molecular orientation in solution [28]. In inorganic crystallization a similar difference may be ascribed to the activation energy barrier. In protein, an essential entropic barrier should exist [33]. The errors in this attachment of conformationally changed species, dimers, trimers and other inhomogeneities and impurities, e.g. small molecules in sufficient amount, may induce lattice strain, disorder and thus lower structural resolution [29, 30].

9. Adsorption and solubility–theoretical approach

The coverage of a step with unit cells, $\theta = 6.5 \times 10^{-6}$, extracted from the 1D nucleation rate in equation (16) provides a possibility to determine the adsorption density of individual molecules at the steps and terraces and to compare it with theoretical estimates.

In these estimates we should take into account both the energy and the entropy change associated with adsorption. When adsorbed, a molecule loses the high freedom of translation and rotation that it has in a liquid. It is now allowed only to vibrate translationally and rotationally (we ignore here changes in internal motions of atoms and even groups building this molecule). In other words, the adsorbed molecule is confined in a much smaller volume of the phase space, since its coordinate and velocity ranges are now limited, as compared to the bulk solution, despite the 'wish' of the temperature to expand the occupied phase space. Thus, adsorption is associated with decrease of both translational and rotational entropy. The stronger this limitation, the larger is the loss of entropy due to adsorption and the corresponding increase of the free energy or chemical potential. The thermodynamic quantity that takes care of the system spread in the phase space and thus of its entropy and energy is the partition function, Z. In what follows, the partition function of the large protein molecules in ideal gas will be used, having in mind that the ideal gas approximation for the dilute solution is well known to provide the correct equation of state, i.e. osmotic pressure as a function of concentration and temperature. We assume that this approximation describes some features of rotational entropy also. Indeed, the Brownian translational and rotational motions of a macromolecule in a liquid are characterized by average energy $kT/2$ per degree of freedom, despite damping of macroscopic motions by the solvent. To that accuracy, the distribution of states in the phase space of coordinates and (both translational and rotational) velocities for the macromolecule in solution are similar to the distribution in an ideal gas.

The standard translational partition function of a particle (the protein molecule) in ideal solution or gas [31] is:

$$Z_t = e/C\Lambda^3 \qquad \Lambda \equiv h/(2\pi mkT)^{1/2} \tag{18}$$

where C is the protein molecule concentration is solution (cm^{-3}), Λ is the de Broglie wavelength of the molecule, m is the molecule mass, $h = 6.62 \times 10^{-27}$ erg is the Planck constant, $k = 1.36 \times 10^{-16}$ erg K^{-1} is the Boltzman constant, T is the temperature. The rotational partition function of an asymmetric molecule in a gas is [31]

$$Z_r = \sqrt{\pi}(8\pi^2 kTI)^{3/2}/h^3 \tag{19}$$

where I is the moment of inertia of the (spherical) molecule. Partition functions for translational and rotational vibrations should be taken in the high temperature approximation, $h\nu \ll kT$:

$$Z_{vt,vr} = (kT/h\nu_{t,r})^3. \tag{20}$$

Here the translational (t) and rotational (r) vibration frequencies,

$$\nu_t = (1/2\pi)(K/m)^{1/2} \qquad \nu_r = (1/2\pi)(K_r/I)^{1/2} \tag{21}$$

are supposed to be equal for the three directions of translation and the three axes of rotation. In equation (21), K (erg cm^{-2} = dyn cm^{-1}) and K_r (erg) are the force constants for the t and r vibrations.

If we ignore internal degrees of freedom of the macromolecule, its chemical potentials in the liquid solution (l) and in the adsorbed state (a) are:

$$\mu_l = -kT \ln[Z_t Z_r / e] + \varepsilon_l \tag{22}$$

$$\mu_a = -kT \ln[Z_{vt} Z_{vr} / \theta_1] + \varepsilon_a \tag{23}$$

where the partition functions are given by equations (18)–(21) while ε_l and ε_a are the potential energies in the l and a states and θ_1 is the step coverage by single molecules. Equilibrium coverage follows from the equality $\mu_l = \mu_a$:

$$\theta_1 = C(\Lambda^3 Z_{vt} Z_{vr} / Z_r) \exp(2\varepsilon_0 / kT). \tag{24}$$

Taking $2\varepsilon_0 = \varepsilon_l - \varepsilon_a$, we have chosen a simple cubic lattice approximation of the orthorhombic lysozyme of which the actual structure is shown in figures 6(a), (b) in projections to the ab and the bc planes respectively [27]. The unit cell includes four molecules and each molecule in the crystal bulk has six nearest neighbours. Its macrobonds A, B, C with the neighbours consist of several hydrogen and van der Waals bonds. However, binding between the molecules 3 and 4 is missing (figure 6(a)) and the whole arrangement is not simple cubic. Nevertheless, we simplify this structure to simple cubic of the type shown in figure 6(c). Thus we 'average' molecular states over the unit cell. However, we keep the real feature of the lattice by considering the whole unit cell of four molecules as a growth unit for 1D nucleation (section 5) and the kink as formed also by the whole unit cell. Actually, single molecules are supposed to be attached and detached, so that both complete and incomplete unit cells are present at the step. Considering the 1D nucleation, we ignored simultaneous building of two neighbouring unit cells and the corresponding possibility of a faster nucleation process.

In the simple cubic lattice approximation, adsorption of a molecule at the step is associated with formation of two bonds of energy ε_0 each: thus, in equation (24), $2\varepsilon_0 = \varepsilon_l - \varepsilon_a$. Substituting equations (18)–(21) into equation (24) one obtains the coverage of the step by single molecules along the re-entrant angle (the state 'Mol' in figure 6(c)):

$$\theta_1 = \pi C (kT/\tilde{K})^3 \exp(2\varepsilon_0 / kT) \qquad \tilde{K} \equiv (K K_r)^{1/2}. \tag{25}$$

This coverage θ_1 does not explicitly depend on molecular mass, moment of inertia or molecular size. However, the effective force constant, $\tilde{K}$, does depends on the type, strength and extension of the intermolecular contacts. Both ε_0 and $\tilde{K}$ are parameters to be found from comparison with experiment.

Arrangement of four molecules from the position 'Mol' at the step to the 'Cell' configuration at the step (figure 6(c)) does not change the number of unsaturated bonds, since one bond can be ascribed to one face of the single cubic molecule. Therefore, probability of finding a unit cell at the molecular step site, like any aggregate of four molecules of the same energy, is

$$\theta = \theta_1^4. \tag{26}$$

This equation links equation (25) to the experimental coverage θ of the step by the cells, equation (16).

The second equation to determine the parameters ε_0 and $\tilde{K}$ is the solubility equation. It is based on the well known fact that the chemical potential of a molecule in any kink position is equal to its chemical potential in the crystal and, at equilibrium, should be equal to the chemical potential of the molecule in the solution. For complex lattices with the unit cells

formed by several molecules occupying non-equivalent positions, this statement is not correct since only the unit cells as whole may form repeatable real kink positions. Nevertheless, as mentioned above, to build a general qualitative framework, we average the states of various non-equivalent molecules in the cell. Within this approximation, the molecule '1' in figure 6(c) is in the 'kink' position i.e. it is bound by three bonds of an average strength, though this is not the actual kink built of four molecules. We assume also that the vibration frequencies in this 'kink' and at the step do not differ much one from another. Then, similarly to equation (25) one can write the simple equation for solubility, C_e:

$$C_e = \pi^{-1}(\tilde{K}/kT)^3 \exp(-3\varepsilon_0/kT) \tag{27}$$

where $3\varepsilon_0$ is the cell-averaged detachment energy of a single molecule from the 'kink' in the unit cell.

At $kT = 4 \times 10^{-14}$ erg, equations (24)–(27) provide the experimental coverage $\theta = 6.5 \times 10^{-6}$ and concentration $C_e = 1.05 \times 10^{-18}$ cm^{-3} at $\varepsilon_0 = 2.2$ kcal mol^{-1} ($\varepsilon_0/kT \simeq 3.68$) and $\tilde{K} = 2.3 \times 10^{-6}$ dyn. The apparent enthalpy of crystallization is thus $3\varepsilon_0 \simeq 6.6$ kcal mol^{-1}. This is rather close to the enthalpy of 7.6 kcal mol^{-1} following from the data of [32]. Keeping the same approximations for the partition function of a molecule in the 'kink' 1 (figure 6(c)), at the step ('Mol', figure 6(c)) and on the terrace, we obtain the terrace coverage at the bulk concentration C

$$\theta_s = \pi(kT/\tilde{K})^3 C \exp(\varepsilon_0/kT) \tag{28}$$

and the coverages at the crystal-solution equilibrium, $C = C_e$:

$$\theta_{1e} = \exp(-\varepsilon_0/kT) \qquad \theta_{se} = \exp(-2\varepsilon_0/kT). \tag{29}$$

The simplicity of expressions for solubility and coverages as well as the absence of the pre-exponential factors in equation (29) come from the assumption that the vibration states in the 'kink', at the step and on the terrace are identical. In real situation, the prefactors, e.g. ratios of different $\tilde{K}$ should appear along with different bond strengths and influence of the solvent. Therefore one should remember that this approach is aimed only at building a general framework of protein adsorption and solubility. In this model, dependence on pH and nature of solvent comes through ε_0 and $\tilde{K}$. A natural consequence of equation (29) is that the higher is binding energy ε_0 in kT units, the lower the coverage as a result of lower solubility.

Since the real kink energy is $4(\varepsilon_0/2) = 2\varepsilon_0$, the equilibrium interkink distance is [4, 5]:

$$x_0 = (c/2)[2 + \exp(2\varepsilon_0/kT)] = 792\ c = 2.42 \times 10^{-4}\ \text{cm}. \tag{30}$$

Therefore, indeed, the step should be straight with only one kink per 792 lattice spacings. Transition from this equilibrium to the actually measured interkink distance includes equation (26), which takes care of the complex structure of the lattice. This equilibrium average interkink distance is naturally larger than 188 c following from table 1 supporting the essentially kinetic nature of the observed kink density.

There are no data to judge the average force constant, $\tilde{K}$. For simple CH, CF, CCl, CNO_2 bonds the valence (stretching) force constant $K \simeq (3\text{–}5) \times 10^5$ erg cm^{-2} [34]. The force constants change the angles between the bonds in the CCC, CCH, HCH, CCl, CCCl, HCO, CCN molecules are within the range $(0.5\text{–}1) \times 10^{-11}$ erg. Thus the artificial combination formally analogous to $\tilde{K}$ is $\sim(1\text{–}2) \times 10^{-3}$ dyn, three orders of magnitude larger than the $\tilde{K}$ from equations (26) and (27). The difference may be ascribed to the different nature of the binding. Specifically, it might come from the shallower potential well describing the extended complex intermolecular protein contact, in particular with respect to rotation or gliding of one molecule over the other, from the softer binding at the kink and step positions as compared to

the bulk and, of course, from approximations used to obtain equations (25) and (27). With the force constant $\tilde{K} \simeq 2.10^{-6}$ dyn, one might expect vibration frequencies of 10^9–10^{10} s^{-1}, i.e. in the radio frequency range.

Equation (27) gives general predictions for solubilities in macromolecular systems with different binding energies. At strong binding, $\varepsilon_0/kT > 1$, one should expect a conventional exponential increase of solubility with temperature. At $\varepsilon_0/kT < 1$, the solubility should be retrograde, decreasing with increasing temperature: the large entropy increase associated with dissolution prevails over the smaller loss in potential energy.

Coverage of a terrace with adsorbed molecules follows from equation (28) as 1.3×10^{-3}. If this figure is close to reality, one should not expect an essential contribution to growth from surface diffusion even if it exists in the adsorbed layer: the volume fraction of protein in the bulk solution $C\omega \simeq 6.3 \times 10^{-2}$, i.e. is essentially larger than the surface coverage.

The surface energy per unit area at the ⟨001⟩ step riser is $\simeq \varepsilon_0/bc = 0.7$ erg cm^{-2}, close to $\sim$1.2 erg cm^{-2} for free energy on the (110) face of tetragonal lysozyme. However, the energy per molecular site in kT units is $\varepsilon_0/2kT \simeq 1.84$, exceeding $\sim$1.3 for tetragonal modification where the steps are indeed far less polygonized. Of course strong anisotropy in binding [27] should be the determining factor making the ⟨001⟩ step straight.

10. Summary and conclusions

Straight elementary growth steps along the ⟨001⟩ direction on the (010) face of orthorhombic lysozyme moving away from the edge between the (010) and (110) faces were observed being generated by a flat-top excrescence along the ⟨001⟩ edge between the 010 and (110) faces (figure 5). Single elementary kinks corresponding to the row of unit cells along the c-axis have been directly seen and studied. The step height and kink width are close to the lattice spacing $b = 7.37$ and $a = 5.64$ nm, respectively. Thus each kink riser should consist of four molecules, the number of molecules per unit cell.

Statistics of 269 kinks of the both positive and negative signs were collected and the step rate was measured to be 0.19 nm s^{-1} at the supersaturation $C/C_e \simeq 2$. The kink rate evaluated from the step rate and the kink density was found to be 19 nm s^{-1}. This is equivalent to the attachment of 12.6 cells s^{-1} and detachment of 6.3 cells s^{-1}. Since the unit cell is built of four molecules these fluxes are equivalent, on average, to 50.4 and 25.2 molecules s^{-1} attaching to and detaching from the kink. The estimated Brownian attempt frequency to join a kink site from solution is estimated to be 10^8 s^{-1}. The difference is believed to occur because of tough statistical selection of large asymmetric molecules in solution before they are attached to the lattice. Kinetic coefficients for steps and kinks were found to be $\beta_{st} = 6 \times 10^{-7}$ cm s^{-1}, $\beta_k = 6 \times 10^{-5}$ cm s^{-1}. The latter qualitatively fits with $\beta_k \simeq 2 \times 10^{-5}$ cm s^{-1} estimated from the β_{st} for rounded steps on the (101) face of the tetragonal lysozyme. The one-dimensional (1D) nucleation rate was also evaluated from the step rate and kink statistics to be $J = 2.7 \times 10^{-5}$ nm^{-1} s^{-1}. The 1D nucleation rate was outlined by the conservation function technique for the nucleus consisting of two unit cells, the unit cell being considered as a building unit at the step. The corresponding equation for J allowed us to evaluate experimental coverage of the step unit sites by the completed unit cells to be 6.5×10^{-6}.

Simple equations for adsorption and solubility have been derived taking into account the partition function of a macroparticle both in an ideal gas and in the adsorbed state. Confronting these equations with experiment an apparent dissolution enthalpy of $\Delta H = 6.6$ kcal mol^{-1} was found for the orthorhombic modification, not far from the experimental value of 7.6 kcal mol^{-1} [32]. The theoretical solubility is found to be proportional to $T^{-3} \exp(-\Delta H/kT)$ predicating

a mainly exponential increase at $\Delta H/kT > 3$ and retrograde solubility at $\Delta H/kT < 3$ ($\Delta H < 1.8$ kcal mol^{-1}). The coverage of the step riser by single molecules is expected to be $(6.5 \times 10^{-6})^{1/4} \simeq 5 \times 10^{-2}$.

Acknowledgments

This work was supported jointly by NASA grants NCC8-66-050 and NAG8-1454, by agreement between MSU and AMMSA/MSFC No 03537-00-009, and by grant No 37-03-32778a of the Russian Foundation for Basic Research.

The authors highly appreciate the technical assistance of Ms S Zarger.

References

[1] Kossel W 1927 *Nachr. Ges. Wiss., Gottingen, Math-Phys. Kl* p 135
[2] Stranski I N 1928 *Z. Phys. Chem.* **136** 259
Stranski I N and Kaishev R 1934 *Z. Phys. Chem.* B **26** 317
Stranski I N and Kaishev R 1935 *Phys. Z.* **36** 393
[3] Kaishev R 1981 *J. Cryst. Growth* **51** 643
[4] Burton W, Cabrera N and Frank F 1951 *Phil. Trans.* A **243** 299
[5] Chernov A A 1984 *Modern Crystallography III, Crystal Growth (Springer Series Solid State 36)* (Berlin: Springer)
[6] Chernov A A 1989 *Contemp. Phys.* **30** 251
[7] Vekilov P G 1993 *Progress in Crystal Growth and Characterization* **26** 25
[8] Kuznetsov Yu G, Malkin A J, Greenwood A and McPherson A 1995 *J. Struct. Biol.* **114** 184
[9] Land T A, Martin T, Potapenko C, Palmore G T and De Yoreo J J 1999 *Nature* **399** 442–5
[10] Teng H H, Dove P M, Orme C A, De Yoreo J J 1998 *Science* **282** 724–7
[11] Onuma K, Ito A, Tabe I and Teteishi T 1997 *J. Phys. Chem.* B **101** 8534
[12] Chernov A A 1998 *Acta Crystallogr.* A **54** 859
[13] Chernov A A 1995 *Texts and Abstracts, Int. Workshop at ICCBM-6, part 1: Biological Macromolecular Crystallization: Theory and Techniques (Sunpia Fukuyama, 1995)* p 6
[14] Land T A, Malkin A J, Kuznetsov Yu G, McPherson A and DeYoreo J J 1995 *Phys. Rev. Lett.* **75** 2774
[15] Kuznetsov Yu G, Malkin A J and McPherson A 1999 *J. Cryst. Growth* **196** 489
[16] Rashkovich L N, Gvozdev N and Yaminski I V 1998 *Crystallogr. Rep.* **43** 696
[17] Voronkov V V 1970 *Sov. Phys.–Crystallogr.* **15** 8
[18] Voronkov V V 1973 *Sov. Phys.–Crystallogr.* **18** 19
[19] Frank F C 1974 *J. Cryst. Growth* **22** 233
[20] Cristoffersen J and Cristoffersen M R 1988 *J. Cryst. Growth* **87** 41
[21] Zhang J and Nancollas G H 1990 *J. Cryst. Growth* **106** 181 (1990).
[22] Chernov A A 1998 *Theoretical and Technological Aspects of Crystal Growth* ed R Fornari and C Paorichi (Trans Tech Publ Ltd, Switzerland, Germany, UK, USA) p 71
[23] Chernov A A 1970 *Sov. Phys.–Usp.* **13** 528
[24] Cervelle P B, Cesbron F, Berthou J and Jolles P 1974 *Acta Crystallogr.* A **30** 645
[25] Ataka M and Asai M 1988 *J. Cryst. Growth* **90** 86
[26] Guilloteau P, Riess-Kautt M M and Ducruix A F 1992 *J. Cryst. Growth* **122** 223
[27] Oki H, Matsuura Y, Komatsu H and Chernov A A 1998 *Acta Crystallogr.* D **55** 114
[28] Chernov A A 1997 *Phys. Rep.* **288** 61
[29] Chernov A A 1997 *J. Cryst. Growth* **174** 354
[30] Chernov A A 1999 *J. Cryst. Growth* **196** 524
[31] Landau L D and Lifshits E M 1980 *Statistical Physics* 3rd edn part 1; *Course of Theoretical Physics* vol 5, ed E M Liftshits and L P Pitaevski (Oxford: Pergamon)
[32] Shall C A, Riley J S, Li E, Arnold E and Wiencek J M 1996 *J. Cryst. Growth* **65** 290
[33] Chernov A A and Komatsu H 1995 *Science and Technology of Crystal Growth* ed J P. van der Eerden and O S L Bruinsma (Doredrecht: Kluwer) pp 67, 329
[34] Gordon A J and Ford R A 1972 *The Chemist's Companion* (New York: Wiley)